*29th EPS Conference on Plasma Phys. and Contr. Fusion Montreux, 17-21 June 2002 ECA Vol. **26B**, P-2.040 (2002)*

Localized Impurity Sources in JET D and He-fuelled Discharges

K D Lawson, Y Andrew, J H Brzozowski[c], I H Coffey[a], M E Fenstermacher[b], G F Matthews, M F Stamp, and contributors to the EFDA-JET work programme

EURATOM/UKAEA Fusion Association, Culham Science Centre, Abingdon, OX14 3DB, UK
[a]QueensUniversity, Belfast, BT7 1NN, UK
[b]Lawrence Livermore National Laboratory, Livermore, California, USA
[c]Fusion Plasma Physics (Association EURATOM-VR), Alfvén Laboratory, Royal Institute of Technology, SE-10044 Stockholm, Sweden

1. Introduction

An understanding of impurity sources and the transport in the plasma edge and divertor is crucial, if the core impurities in JET and next step machines are to be controlled. The main source of the core impurities is expected to be the divertor, whose surfaces are subjected to high heat and particle fluxes. In JET, these and many other plasma facing surfaces are C tiles. In D plasmas, significant emission from C is also observed along the lower inner wall, suggesting a possible additional source of impurities. Recent experiments in JET, in which the fuel and Neutral Beam Injection (NBI) was changed from D to He, show marked differences in impurity emission. Comparisons of the D and He-fuelled discharges will allow further understanding of the impurity release mechanisms. In particular, the relative importance of physical and chemical sputtering can be assessed, as can the importance of sources outside the divertor. The impurity radiation from comparable L-mode, D and He-fuelled discharges is described. Initial transport simulations have been carried out for two discharges, one D-fuelled and the other predominately He, using the EDGE2D/NIMBUS fluid/Monte Carlo code [1].

2. Experiments

Series of 2.4T, 2.5MA, D and He-fuelled discharges have been analysed, in which the NBI additional heating power and plasma density were varied. The confinement effects the edge region of the plasma and, in this paper, L-mode discharges are considered, the maximum NBI power being ~9MW. Figure 1 shows bulk parameters for the 2 pulses modelled, 50414 (D) and 53981 (He), which are typical of the pulses being considered.

A poloidally scanning VUV spectrometer, which observes both the lower inner wall and the divertor provides valuable data on the spatial distribution of the impurity sources. The range of its line of sight is shown, together with the plasma configuration, in figure 2. This spectrometer records 2 spectral line intensities within the spectral range 200 to 1550Å, with a spatial scan duration of 24ms and an integration time of 0.14ms. Visible spectrometers

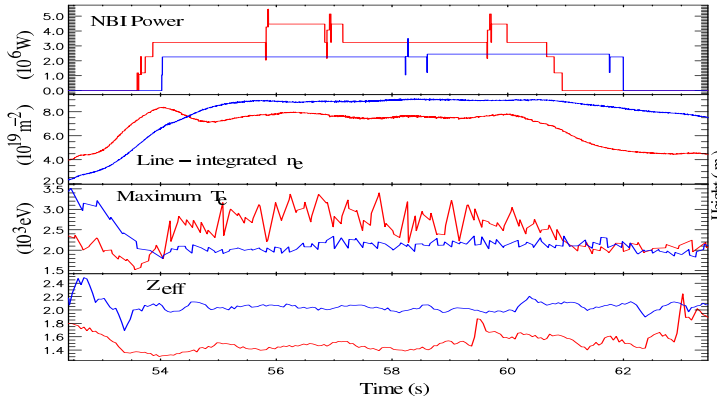

Figure 1. NBI power, line-intergrated n_e, maximum T_e and Z_{eff} for D pulse 50414 (red) and He pulse 53981 (blue) used in the EDGE2D simulations.

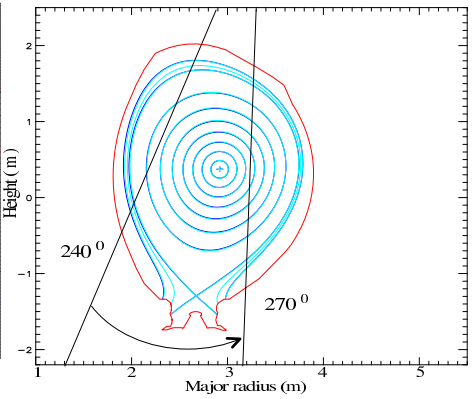

Figure 2. The magnetic configurations of pulses 50414 (D) and 53981 (He), also showing the extreme positions of the VUV spectrometer's poloidal scan.

with fixed lines-of-sight and an infrared camera viewing the divertor box provided additional spectroscopic information. Sweeping the strike points up the vertical target plates enabled good edge temperature and density profiles to be measured with the target tile langmuir probes.

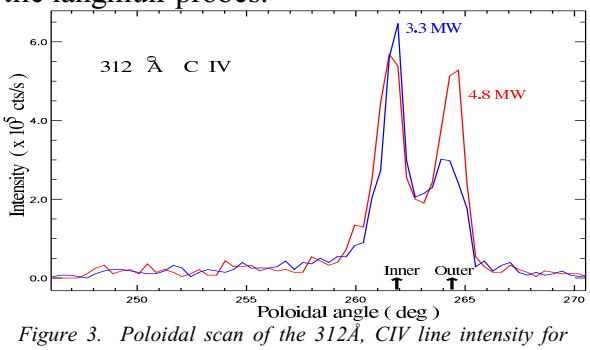

Figure 3. Poloidal scan of the 312Å, CIV line intensity for pulse 50420 at 58.8s (red) and 54.3s (blue) showing the power dependence in D plasmas.

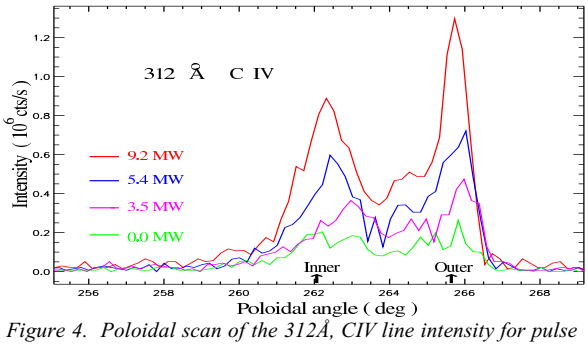

Figure 4. Poloidal scan of the 312Å, CIV line intensity for pulse 53977/57.6s (green), 53986/57s (magenta), 53982/57.5s (blue) and 53986/61s (red) showing the power dependence in He plasmas.

3. Results

An asymmetry in the radiation from the inner and outer divertor regions is observed, in D pulses that from the inner divertor dominating, in He, if an asymmetry is observed, the outer divertor dominating. Figures 3 and 4 show typical poloidal scans of C emission in D and He plasmas, respectively. These diagrams also show the power dependence of the C emission for line-integrated n_e of 8.1 (D) and ~10x10^{19}m^{-2} (He). If physical sputtering is the dominant release mechanism, a power dependence would be expected. Ratios of emission from different C ionisation stages are given in table 1.

D Pulses

		CII		CIII		CIV	
Pulse	Power(MW)	Inner	Outer	Inner	Outer	Inner	Outer
50420	4.8	0.9	1.5	1.0	1.3	0.9	1.8
50420	3.3	1.0	1.0	1.0	1.0	1.0	1.0

He Pulses

		CII		CIII		CIV	
Pulse	Power(MW)	Inner	Outer	Inner	Outer	Inner	Outer
53986	9.2	3.5	5.0	3.6	4.8	4.5	5.9
53982	5.4	1.9	2.4	4.1	3.9	3.1	3.3
53986	3.5	1.3	2.4	1.8	2.3	1.9	2.1
53977	0.0	1.0	1.0	1.0	1.0	1.0	1.0

Table 1. Ratios of the peak emission of CII, CIII and CIV, from the inner and outer divertor.

In D pulses, there is a marked effect with density, illustrated in figure 5 for CII emission. The intensity in the outer divertor and from close to the inner wall increases and the inner and outer divertor peaks merge with increasing density. It is noted that the divertor peaks are more distinct for the lower ionisation stages (figure 6). In He pulses, there is a modest increase in the C divertor emission, although little change along the inner wall (figure 7) and this despite the extreme He emission from this region (figure 8).

The ratio of the C intensities when the fuel is changed from D to He is given in table 2. These are for 3 pulses with a line-integrated n_e of ~9x10^{19}m^{-2}, the NBI power of a D pulse being intermediate to those of two He discharges. A large reduction is seen for the inner divertor signals, particularly for the lowest ionisation stage, whereas that for the outer divertor signals is ~2. This large difference requires an additional release mechanism in the inner divertor region of D plasmas, such as chemical sputtering.

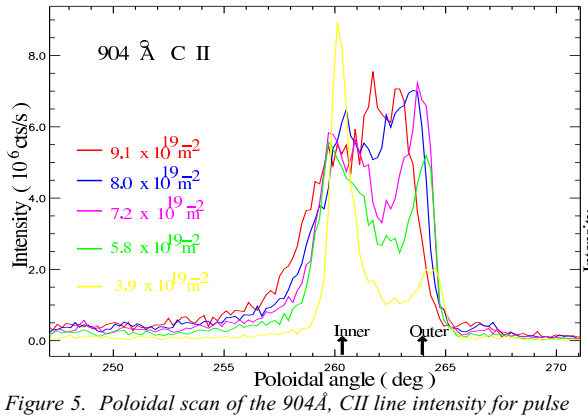

Figure 5. Poloidal scan of the 904Å, CII line intensity for pulse 52690 at 56s (yellow), 57s (green), 58s (magenta), 59s (blue) and 60s (red) showing the density dependence in D plasmas.

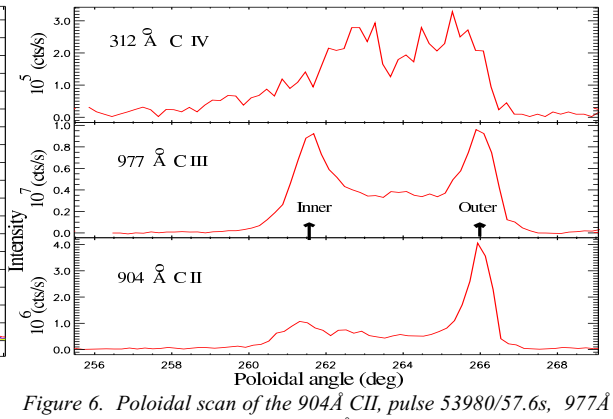

Figure 6. Poloidal scan of the 904Å CII, pulse 53980/57.6s, 977Å CIII, pulse 53978/57.5s and 312Å CIV line intensities, pulse 53986/55s, observed in He plasmas.

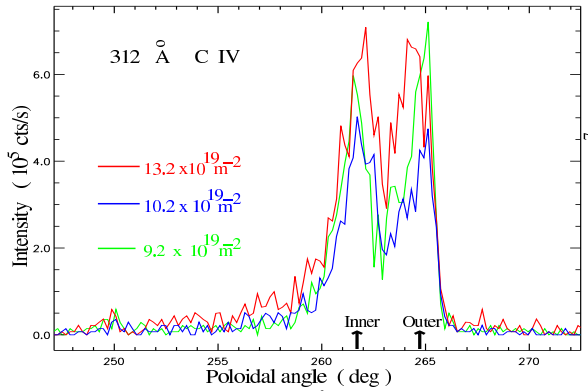

Figure 7. Poloidal scan of the 312Å, CIV line intensity for pulse 53982/57.5s (green), 53977/55.8s (blue) and 53983/57.5s (red) showing the C density dependence in He plasmas.

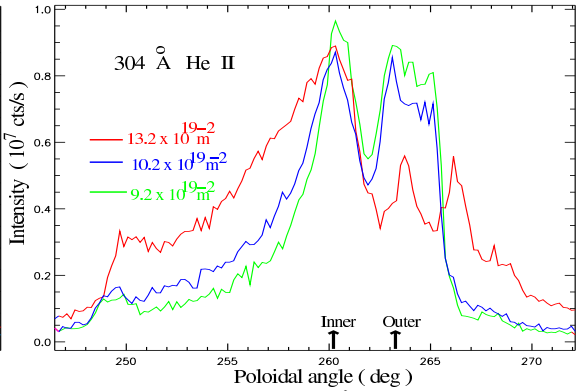

Figure 8. Poloidal scan of the 304Å, HeII line intensity for pulse 53982/57.5s (green), 53977/55.8s (blue) and 53983/57.5s (red) showing the He density dependence in He plasmas.

			CII		**CIII**		**CIV**	
Pulse	Fuel	Power(MW)	Inner	Outer	Inner	Outer	Inner	Outer
50414	D	3.2	1.0	1.0	1.0	1.0	1.0	1.0
53981	He	2.5	0.04	0.58	0.09	0.43	0.15	0.39
53985	He	4.2	0.05	0.68	0.16	0.58	0.18	0.49

Table 2. Reduction in peak emission of CII, CIII and CIV, from the inner and outer divertor.

4. Modelling

Initial simulations have been carried out for two pulses, 50414 (D) and 53981 (He), using the EDGE2D/NIMBUS fluid/Monte Carlo code [1]. This complements the analysis carried out for these pulses using the UEDGE code [2]. In simulations of the D pulse 50414, those including both physical [3] and chemical sputtering [4] indicate a distinct impurity ionization source along the lower inner wall (figure 9). This source is absent when only physical sputtering is included in the simulation (figure 10). The sources in the physical sputtering case are lower by typically a factor of 4 in the divertor region in this comparison. In the plasma edge, this factor is higher, ~12. In simulations for pulse 53981, the He ionization source is seen to extend along the lower inner wall (figure 11), whereas that for the C impurity is localized in the divertor (figure 12). This is consistent with the data presented in figures 7 and 8. With these first simulations, it has not been possible to demonstrate differences in the dominant release mechanisms between the inner and outer divertor in D plasmas. Further optimisation of the EDGE2D runs are required to achieve this and comparisons with the UEDGE results will provide a useful validation of the codes.

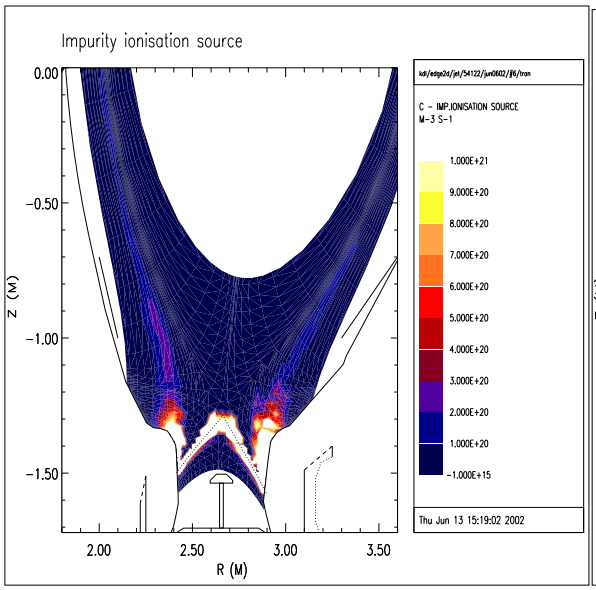

Figure 9. C impurity ionisation source in a simulation of pulse 50414 (D), including both chemical and physical sputtering models.

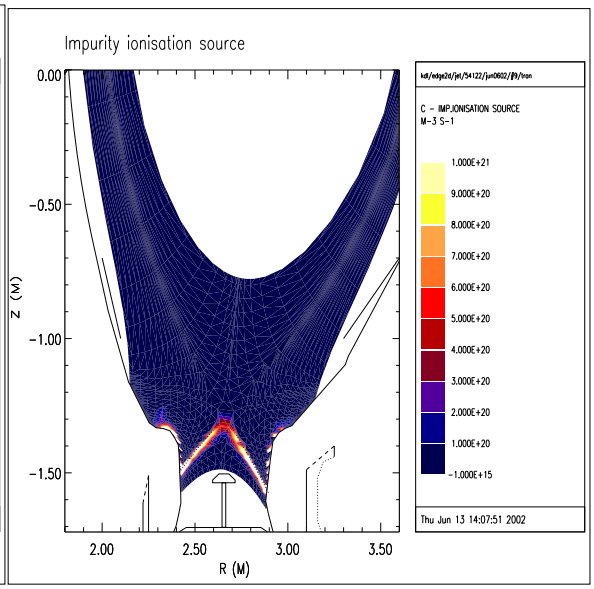

Figure 10. C impurity ionisation source in a simulation of pulse 50414 (D), including only a physical sputtering model.

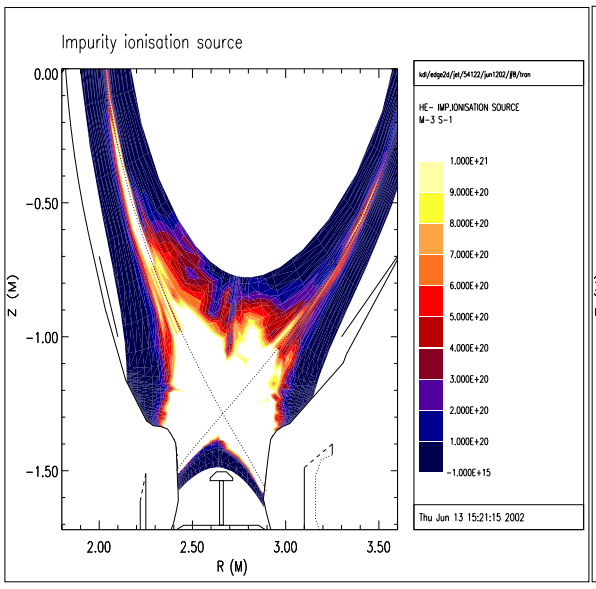

Figure 11. He ionisation source in a simulation of pulse 53981 (He).

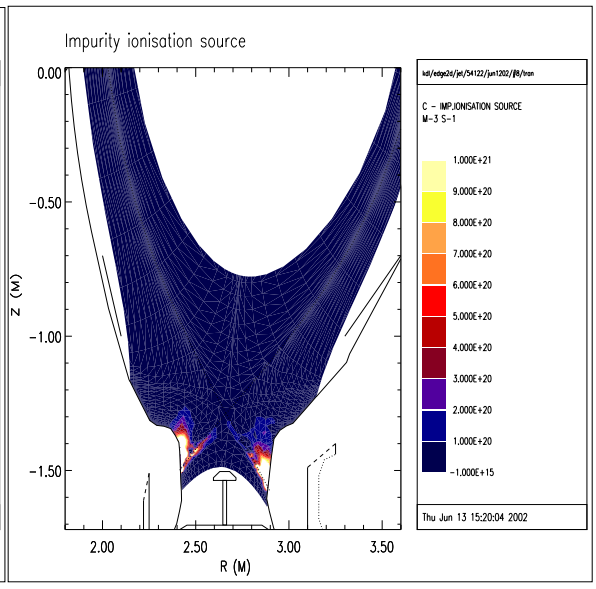

Figure 12. C impurity ionisation source in a simulation of pulse 53981 (He).

[1] R Simonini *et al.*, Contrib. Plasma Phys., **34,** 368, 1994
[2] M E Fenstermacher *et al.*, Presented at the 15th PSI Conf., Japan
[3] W Eckstein *et al.*, IPP 9/82, 1993 [4] A A Haasz *et al.*, J. of Nuc. Mat., **248**, 19, 1997

It is a pleasure to thank G Corrigan, M O'Mullane and T O'Neill for help in the preparation of this paper. This work was performed under the European Fusion Development Agreement and is partly funded by EURATOM and the UK Department of Trade and Industry